Entanglement Effects in Semiflexible Polymer Solutions. 3. Zero-Shear Viscosity and Mutual Diffusion Coefficient of Poly(*n*-hexyl isocyanate) Solutions

Atsuyuki Ohshima,† Aya Yamagata, and Takahiro Sato*,‡

Department of Macromolecular Science, Osaka University, 1-1 Machikaneyama-cho, Toyonaka, Osaka 560-0043, Japan

Akio Teramoto

Research Organization of Science and Engineering, Ritsumeikan University, and CREST of Japan Science and Technology, Nojihigashi 1-1-1, Kusatsu, Siga, Japan

Received June 10, 1999; Revised Manuscript Received September 30, 1999

ABSTRACT: To critically compare with the fuzzy-cylinder-model theory for the dynamics of stiff-chain polymers in solution, zero-shear viscosities and mutual diffusion coefficients have been measured for dilute through concentrated isotropic solutions of poly(*n*-hexyl isocyanate) (PHIC) samples with the number N of Kuhn's statistical segments between 0.21 and 55. The theory describes quantitatively both viscosity data for PHIC samples with N smaller than 20 and diffusion coefficient data for PHIC samples with N up to 26, with a single set of hydrodynamic parameters characteristic of PHIC. This confirms the validity of the theory to explain the global-motion dynamics of semiflexible polymer chains in solution. On the other hand, such a quantitative description is not achieved with zero-shear viscosities for PHIC samples with N larger than 20, where a power-law concentration dependence appears at higher concentrations in a form different from a scaling law seen for flexible polymer solutions. This indicates the limitation of the validity of the fuzzy-cylinder-model theory.

1. Introduction

The zero-shear viscosity η_0 and mutual (or cooperative) diffusion coefficient D_m are basic quantities in the global-motion dynamics of polymer chains in solution. The former is related to the rotational diffusivity, while the latter reflects the translational diffusivity of polymer chains. For flexible polymer solutions, both η_0 and D_m have been extensively studied by many workers to compare with reptation and scaling theories.[1−3]

Sato et al.[4,5] proposed a theory based on the *fuzzy cylinder model*, which deals with both rotational and translational diffusivities of stiff-chain polymers in solution. So far, this theory has been mostly compared with η_0 data of stiff or semiflexible polymer solutions.[4,6−9] For example, we[8,9] have recently demonstrated that this theory is favorably compared with η_0 of dichloromethane (DCM) solutions of a semiflexible polymer, poly(*n*-hexyl isocyanate) (PHIC), in dilute through concentrated isotropic regions unless the molecular weight of PHIC is very high.

To test more critically the validity of the fuzzy-cylinder-model theory, it is essential to examine whether the theory can describe not only η_0 but also D_m data of the same systems consistently. The present study was undertaken to make this test, by choosing PHIC solutions in different solvents as test systems. PHIC is a suitable semiflexible polymer for this critical test, because it is effectively fractionated to obtain samples with narrow molecular weight distributions and also has good solubilities to such convenient organic solvents as toluene, DCM, and *n*-hexane, in which its conformational parameters are known.

This paper presents experimental results of D_m of DCM solutions and η_0 of toluene and *n*-hexane solutions of PHIC and compares those results with the fuzzy-cylinder-model theory. Since the dynamic parameters included in the theory have been already determined in our previous viscometric study[9] of DCM solutions of PHIC, we can unequivocally compare between the theory and experiment both of D_m and η_0.

2. Experimental Section

A. PHIC Samples. Fourteen fractionated PHIC samples were used in this study. Among them, six were the samples used in the previous study,[8] and the rest of the samples were fractions obtained in the same polymerization and fractionation procedures. The weight-average molecular weights M_w were measured by static light scattering for six PHIC samples in dichloromethane (DCM), while the viscosity average molecular weights M_v were estimated for all the samples from the intrinsic viscosity $[\eta]$ in toluene at 25 °C, in *n*-hexane at 25 °C, or in DCM at 20 °C using the established $[\eta] - M_w$ relations.[10,11] (See ref 12 for the detailed procedure of static light scattering.) Table 1 lists the results as well as the polydispersity indices M_w/M_n determined by gel permeation chromatography. The results of M_v almost agree with M_w for the seven PHIC samples, and in what follows, M_v is not differentiated from M_w and both are denoted by M.

The PHIC−*n*-hexane system is known to form a physical gel at low temperatures and high concentrations.[13] For this reason, viscosity measurements for this system were made at 40 °C and limited to concentrations where the physical gelation did not take place. The wormlike-cylinder parameters of PHIC in 40 °C *n*-hexane were determined by fitting the Yamakawa−Fujii−Yoshizaki theory[14,15] to the $[\eta] - M$ relation for five PHIC samples in 40 °C *n*-hexane,[16] with the cylinder diameter d being assumed to be 1.8 nm, which is the d value of PHIC in 25 °C *n*-hexane.[17] The values of the molar mass M_L per unit contour length and the persistence length q determined are listed in Table 2 along with those in 25 °C *n*-hexane,[17] 25 °C

† Present address: Central Laboratory, Rengo Co., Ltd., 186-1-4, Ohhiraki, Fukushima-ku, Osaka 553-0007, Japan.
‡ CREST of Japan Science and Technology.

10.1021/ma9909298 CCC: $18.00
Published on Web 11/24/1999

Table 1. Molecular Characteristics of PHIC Samples Used

sample	M_w (M_v[a])/10^4	N	$[\eta]$/cm^3 g^{-1}	k'	$\langle S^2\rangle^{1/2}$/nm	M_w/M_n	c_I/g cm^{-3} [b]
(a) In 25 °C Toluene							
D-3	(1.15)	0.21	17.9	0.62		1.03	0.36
P-3	(1.9)	0.35	36.4	0.49		1.02	0.28
O-2p	(3.8)	0.69	98.6	0.39		1.02	0.22
N-2	6.7 (7.1)	1.2	227	0.37		1.02	0.20
M-3	(11)	2.0	381	0.36		1.03	0.19
M-2	13.5 (14)	2.5	517	0.37		1.04	0.18$_5$
I-2	25.2 (27)	4.6	983	0.40		1.10	
J-2	48.2 (48)	8.8	1760	0.43			
G-2	(110)	20	3980	0.47			
H-1−2	(300)	55	8490	0.48			
(b) In 40 °C *n*-Hexane							
M-2	13.5	2.5	532	0.38			
C-4	31	5.8	1080	0.36			
JP-2	(140)	26	4700	0.45			
(c) In 20 °C Dichloromethane							
MO-3	7.3 (6.6)	2.3	157	0.37	20.2	1.03	
M-2	13.5 (13)	4.3	320	0.37	29.1	1.04	0.24
C-4	31 (27)	10	621	0.41	47.2		
F-1	(82)	26	1620	0.51	86[c]		

[a] Estimated from $[\eta]$ in toluene (25 °C), *n*-hexane (25 °C), and DCM (20 °C) with the established $[\eta] - M_w$ relations.[10,11] [b] Phase boundary concentration where the nematic phase begins to appear in 25 °C toluene solutions estimated by the interpolation of Itou and Teramoto's data.[54] [c] Value obtained by interpolating Jinbo et al.'s data.[12]

Table 2. Wormlike Cylinder Parameters of PHIC in Different Solvents

solvent	temp/°C	q/nm	M_L/nm^{-1}	d/nm
dichloromethane	20[a]	21	740	1.6
toluene	25[a]	37	740	1.6
n-hexane	25[b]	41	730	1.8
	40	37	735	1.8

[a] Taken from ref 10. [b] Taken from ref 17.

toluene,[10] and 20 °C DCM[10] previously reported. It is seen from the table that q of PHIC in 40 °C *n*-hexane is equal to that in 25 °C toluene but larger than that in 20 °C DCM. The values of the number N of Kuhn's statistical segments, estimated from M by the relation $N = M/2qM_L$, are listed in the third column of Table 1, covering a wide range from 0.21 (rodlike) to 55 (considerably flexible).

B. Viscometry. Shear viscosities η of toluene and *n*-hexane solutions of PHIC samples at 25 and 40 °C, respectively, were measured at different shear rates and polymer concentrations by a magnetically controlled ball viscometer (Iwamato Co., Ltd., Kyoto, Japan) or by a four-bulb low-shear-capillary viscometer, both of which were used in the previous study; see ref 8 for the detailed procedure. Zero-shear viscosities η_0 were obtained by extrapolating η obtained to the zero-shear rate.

C. Dynamic Light Scattering. Mutual diffusion coefficients D_m in DCM solutions of four PHIC samples (MO-3, M-2, C-4, and F-1) were determined as functions of the polymer concentration by dynamic light scattering. Test solutions were prepared in the procedure applied by Jinbo et al.'s in a static light scattering study[12] of the same system, and the normalized autocorrelation function $g^{(2)}(t)$ of scattered light intensity for each solution was measured at 20 °C by a light scattering goniometer (JASCO, Lsp-20) equipped with a photon correlator (Unisoku, DP-200) or by an ALV/DLS/SLS-5000 light-scattering system, with an argon ion laser (NEC, GLG3110) emitting vertically polarized light of 488 nm wavelength λ as light source.

By the Gaussian approximation,[18] $g^{(2)}(t)$ can be related to the dynamic structure factor $\hat{S}(k,t)$ by

$$g^{(2)}(t) = 1 + f\hat{S}(k,t)^2 \tag{2.1}$$

where k is the absolute value of the scattering vector and f is a coherence factor. In this study, $g^{(2)}(t)$ was analyzed by the cumulant method. The first cumulant Γ was determined from $g^{(2)}(t)$ by

$$\Gamma \equiv \lim_{t\to 0} \mathrm{d}(\ln \hat{S}(k,t))/\mathrm{d}t = \frac{1}{2}\lim_{t\to 0} \mathrm{d}(\ln[g^{(2)}(t) - 1])/\mathrm{d}t \tag{2.2}$$

In general, Γ contains contributions of various modes of the polymer dynamics at finite k, but only the translational diffusion mode remains at $k \to 0$.[18,19] Thus, the mutual diffusion coefficient D_m is estimated from Γ by

$$D_m = \lim_{k\to 0} \Gamma/k^2 \tag{2.3}$$

where k is related to the scattering angle θ by $k = (4\pi n/\lambda)\sin(\theta/2)$ with the refractive index n of the solution.

3. Results

A. Zero-Shear Viscosity. Figure 1 shows the double logarithmic plot of the zero-shear viscosity η_0 vs the polymer mass concentration c for toluene solutions of 10 PHIC samples at 25 °C and for *n*-hexane solutions of three PHIC samples at 40 °C. The data points for toluene and *n*-hexane solutions with $M \lesssim 3 \times 10^6$ follow curves concave upward up to c near the concentrations c_I where the nematic phase starts to appear (cf. Table 1). This non-power-law behavior is characteristic of stiff-chain polymer solutions.[5,20−22] However, the data points for the three highest molecular weight samples (H-1−2, G-2, and J-2) in toluene and the highest molecular weight sample (JP-2) in *n*-hexane seem to follow straight lines with the slope ca. 3.2 at higher c regions. Similar power-law behavior was observed previously[8] for dichloromethane (DCM) solutions of high molecular weight PHIC samples, but the exponent was slightly larger (3.6) for the DCM solutions. The power-law behavior is usually observed for entangled flexible polymer solutions, and the concentration dependence of η_0 shown in Figure 1 for PHIC solutions implies the crossover from stiff-chain polymer behavior to flexible polymer behavior.

Figure 2 shows the double logarithmic plot of η_0 vs the molecular weight M for toluene solutions at fixed c. The data points almost follow straight lines with a slope of 4 at high M regions. The same power-law dependence on M was obtained for the DCM solution of PHIC at a high molecular weight region,[8] but the exponent 4 of the toluene and DCM solutions of PHIC is appreciably larger than the well-known exponent 3.4 for solution viscosities of entangled flexible polymers.[1,23] Much larger exponents were reported for such stiffer polymers as schizophyllan[20,21] and xanthan,[22] and this remarkable molecular weight dependence is characteristic of stiff-polymer solutions. The exponent 4 for PHIC solutions indicates that PHIC solutions studied here are not yet in the flexible regime.

Figure 3 compares relative viscosities η_r (i.e., η_0 divided by the solvent viscosity $\eta^{(S)}$) of sample M-2 dissolved in the three different solvents, toluene (25 °C), *n*-hexane (40 °C), and DCM (20 °C). The data for DCM solutions are reproduced from the previous paper.[8] The data points both for the toluene (unfilled circles) and *n*-hexane (filled circles) solutions follow the single solid curve indicated in the figure, but those for the DCM solutions (triangles) deviate downward from this solid curve in an intermediate c range. As mentioned in section 2, PHIC has the same persistence length q (=37 nm) in 25 °C toluene and 40 °C *n*-hexane but a smaller q (=21 nm) in DCM,[10,12] and the other wormlike cylinder

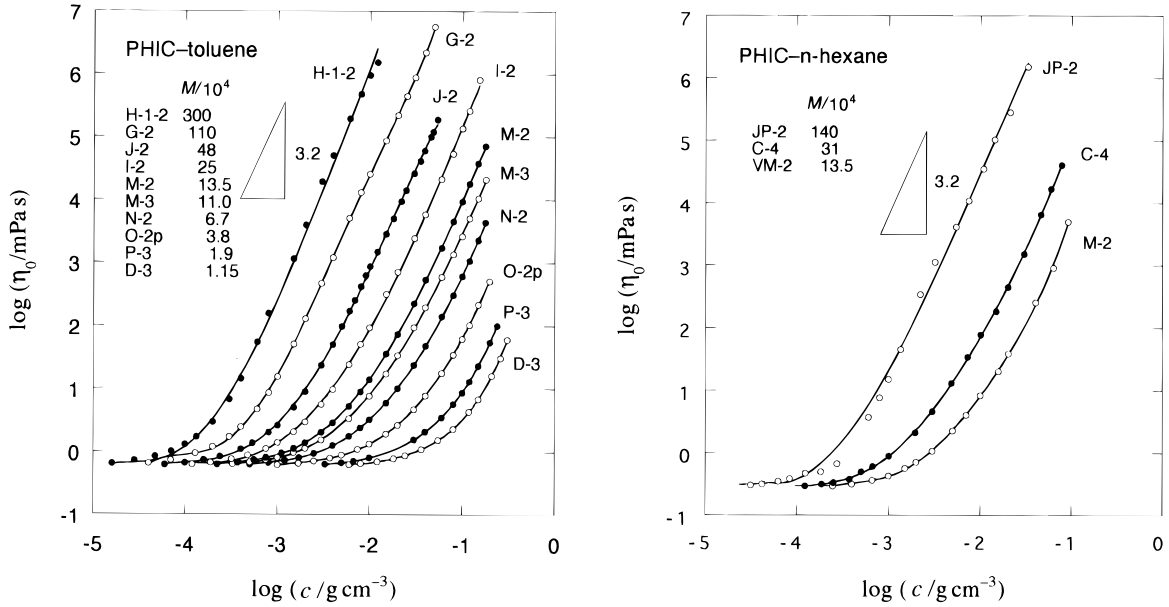

Figure 1. Double logarithmic plots of the zero-shear viscosity η_0 vs the polymer mass concentration c for toluene (25 °C) and *n*-hexane (40 °C) solutions of PHIC samples.

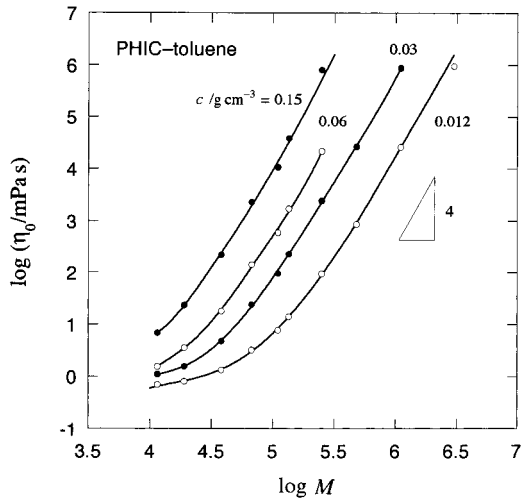

Figure 2. Double logarithmic plots of the zero-shear viscosity η_0 vs the polymer molecular weight M for toluene solutions of PHIC samples at 25 °C.

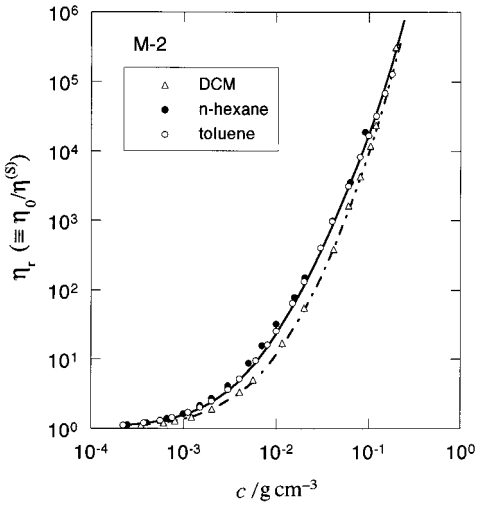

Figure 3. Relative viscosities η_r of sample M-2 ($M = 1.35 \times 10^5$) dissolved in the three different solvents: (●) toluene solutions (25 °C), (○) *n*-hexane solutions (40 °C), (△) DCM solutions (20 °C); solid and dot−dash curves, values calculated by the fuzzy-cylinder-model theory. The data for DCM solutions were taken from ref 8.

parameters (M_L and d) are almost the same in the three solvents (cf. Table 2). The viscosity behavior shown in Figure 3 exactly correlates to these q values in the three solvents.

B. Dynamic Light Scattering. Figure 4 shows the plot of ln $[g^{(2)}(t) - 1]$ against k^2t for a DCM solution of sample C-4 with $c = 3.10 \times 10^{-3}$ g/cm^3 measured at different θ. In the figure, the data points for different θ are shifted vertically by different amounts for the viewing clarity. The data points at each θ follow a concave curve, and the curvature of the curve is stronger for higher θ. Although not shown here, the nonlinearity in $g^{(2)}(t)$ is enhanced with increasing M of PHIC, and it may come from contributions of rotational motions and conformational changes of PHIC chains to the dynamical structure factor.[24] From the initial slope of the plot of ln $[g^{(2)}(t) - 1]$ vs k^2t (as shown by dotted lines in Figure 4), the first cumulant Γ divided by k^2 was estimated according to eq 2.2 for four PHIC samples examined.[25]

Figure 5 displays the k^2 dependence of Γ/k^2 estimated for the highest molecular weight sample F-1 at different c. At low c, Γ/k^2 shows a positive k^2 dependence, but with increasing c the dependence turns to be negative. This trend of the k^2 dependence of Γ/k^2 was also observed but less remarkably for lower molecular weight samples. Russo et al.[26] reported a similar turnover in the k^2 dependence of Γ/k^2 for semidilute poly(γ-benzyl L-glutamate) solutions. Using a dynamical mean-field theory for rodlike polymer solutions, Doi et al.[19] explained this turnover in terms of the contribution of rotational diffusion motions of rodlike polymers to $\hat{S}(k,t)$. It should be noted that for semiflexible polymer solutions, conformational changes of polymer chains may also affect the k dependence of Γ.[24] We use eq 2.3 to determine the mutual diffusion coefficient D_m by extrapolating the plot of Γ/k^2 vs k^2 to zero k^2, thus eliminating the contributions of the rotational motion and conformational change of the polymer chain to $\hat{S}(k,t)$.

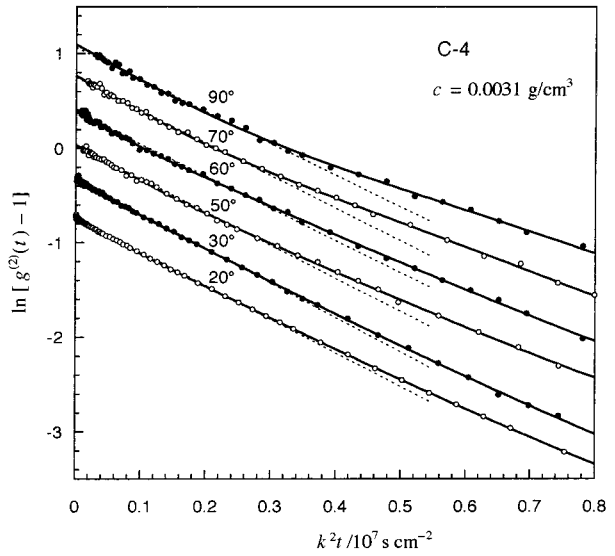

Figure 4. Plots of $\ln[g^{(2)}(t) - 1]$ vs k^2t for a DCM solution of sample C-4 with $c = 3.10 \times 10^{-3}$ g/cm^3 at 20 °C. Data points for different θ are shifted vertically to different amounts for the viewing clarity.

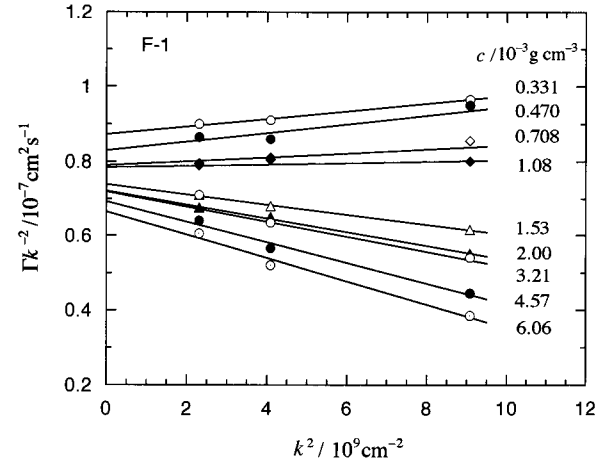

Figure 5. Dependence of Γ/k^2 on k^2 for DCM solutions of sample F-1 with different c.

The results of D_m obtained for the four PHIC samples examined are plotted against c in Figure 6. In panel a, D_m for the two lower molecular weight samples, MO-3 and M-2, are increasing functions of c, and that for the highest molecular weight sample, F-1, is a decreasing function of c. For the intermediate molecular weight sample C-4, D_m tends to level off at higher c. The concentration dependence of D_m is determined by the polymer-chain mobility and thermodynamic force (cf. eq 4.13 in the next section). In good solvents, the former and latter factors are decreasing and increasing functions of c, respectively. It is known that DCM is a good solvent of PHIC,[12] and the results in Figure 6a indicate that the contribution of the thermodynamic force to the concentration dependence of D_m overwhelms that of the mobility at low M, but the situation is opposite for high M.

It is well-known that D_m for semidilute solutions of flexible polymers dissolved in good solvents is an increasing function of c and independent of the molecular weight in the semidilute regime, and its concentration dependence often follows a scaling law.[2] The molecular weight and concentration dependences of D_m for DCM solutions of PHIC, shown in Figure 6a, are remarkably distinct from those for flexible polymers, and they are strongly affected by the chain stiffness.

Translational diffusion coefficients D_0 at infinite dilution for the four PHIC samples were estimated by extrapolating D_m to zero c (cf. Figure 6b), and the results are plotted against M in Figure 7. The solid and dotted curves in the figure show the theoretical values of D_0 for the wormlike-cylinder model calculated according to Yamakawa and Fujii[27] with d = 2.5 and 1.6 nm, respectively, as well as q = 21 nm and M_L = 740 nm^{-1} (cf. Table 2). The data points follow the solid curve for d = 2.5 nm better than the broken curve for d = 1.6 nm which was determined from intrinsic viscosity data of PHIC in 20 °C DCM.[10] The same inconsistent values of d were also obtained from the data of D_0[28] (or the sedimentation coefficient[11]) and $[\eta]$ for PHIC in *n*-hexane[11] as well as for DNA in an aqueous buffer solution.[29] From the chemical structure of PHIC, 2.5 nm for d seems to be too large, but the origin of this unreasonable value is still in dispute.

4. Discussion

A. Fuzzy-Cylinder-Model Theory.[4,5] The basic assumption of this theory is that local conformational changes of a semiflexible chain are much faster than global motions (i.e., the end-over-end rotation and the center-of-mass translation) of the chain even in a concentrated solution. The fast local conformational changes make segments of the chain distribute symmetrically around the chain end-to-end axis, and thus the chain may be modeled by a smoothed density cylinder referred to as the fuzzy cylinder. As a result, global motions of entangled polymer chains can be represented by motions of fuzzy cylinders colliding each other. The effective length L_e and diameter d_e of the fuzzy cylinder are defined by $L_e = \langle R^2\rangle^{1/2}$ and $d_e = (\langle H^2\rangle + d^2)^{1/2}$, where d is the polymer real diameter and $\langle R^2\rangle$ and $\langle H^2\rangle$ are the mean-square end-to-end distance and mean square distance between the chain midpoint and the end-to-end axis, respectively, both of which can be calculated with the persistence length q and the Kuhn segment number N of the polymer chain.[4] In the coil limit, the axial ratio L_e/d_e of the fuzzy cylinder tends to $\sqrt{6}$.

Using this model, Sato et al.[4,5] formulated the rotational, transverse, and longitudinal diffusion coefficients for stiff or semiflexible polymers, as well as the zero-shear viscosity η_0 for their solutions ranging from dilute through concentrated (isotropic) regimes. The entanglement effects on the rotational diffusion coefficient D_r and the transverse diffusion coefficient $D_\perp$ were treated by a mean-field Green's function method, which was originally applied to the rodlike polymer dynamics by Edwards and Evans[30] and Teraoka and Hayakawa.[31,32] The final expressions for D_r and $D_\perp$ read[4,5,9]

$$D_r = \hat{D}_{r0}[1 + \beta_r^{-1/2} L_e^4 f_r(d_e/L_e) c'(\hat{D}_{r0}/6D_{||})^{1/2}]^{-2} \quad (4.1)$$

and

$$D_\perp = \hat{D}_{\perp 0}[1 + \beta_\perp^{-1/2} L_e^4 f_\perp(d_e/L_e) c'(2\hat{D}_{\perp 0}/D_{||})^{1/2}]^{-2} \quad (4.2)$$

where $\hat{D}_{r0}$ and $\hat{D}_{\perp 0}$ are the rotational and transverse diffusivities at switching off the entanglement effects, β_r and $\beta_\perp$ are numerical constants estimated by Teraoka et al. from stochastic geometric arguments by use of the cage model for rodlike polymers to be 1350[33] and 560,[34]

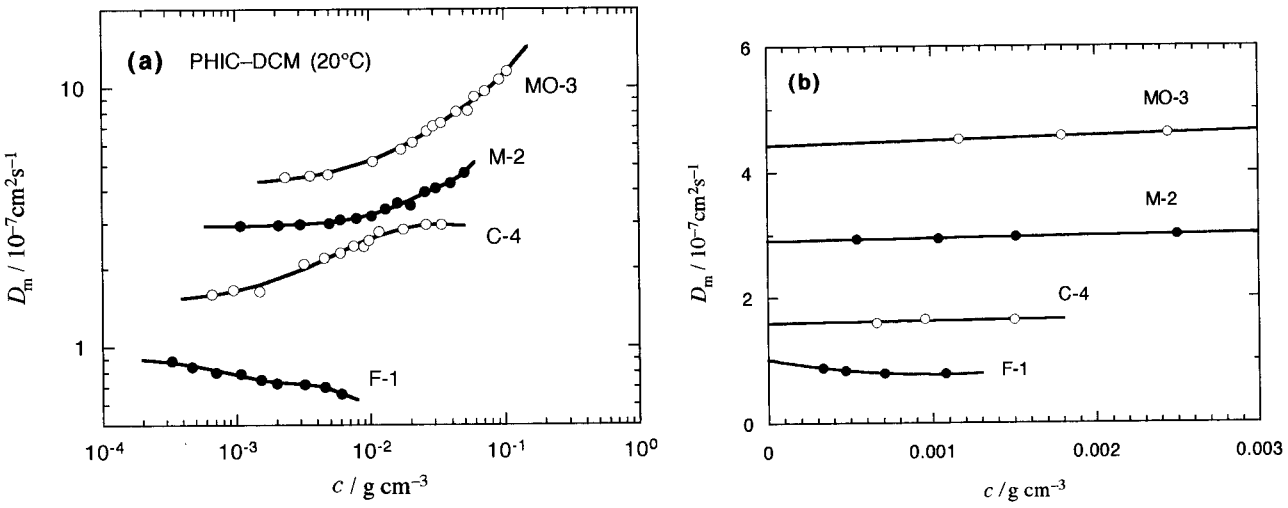

Figure 6. Concentration dependence of the mutual diffusion coefficient D_m for DCM solutions of PHIC.

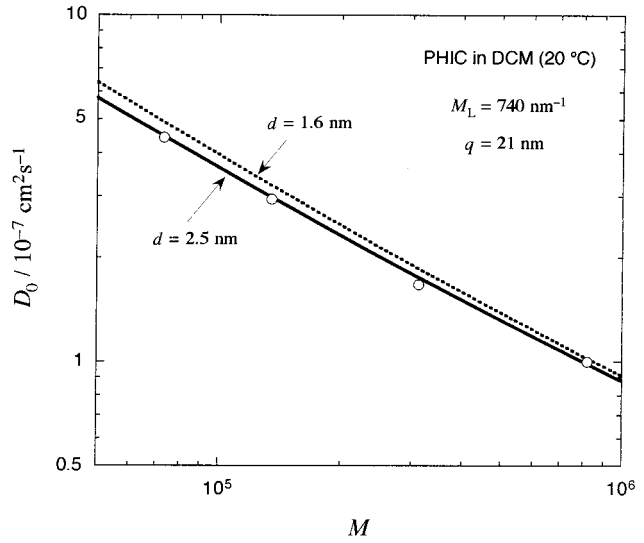

Figure 7. Molecular weight dependence of the translational diffusion coefficient D_0 at infinite dilution: the solid and dotted curves, theoretical values calculated by the Yamakawa-Fujii theory[27] with d = 2.5 and 1.6 nm, respectively.

respectively, and c' is the polymer number concentration. The functions $f_r(d_e/L_e)$ and $f_\perp(d_e/L_e)$ take into account the release of entanglements by fluctuation of the segment distribution in the fuzzy cylinder, and are given by[5]

$$f_r(x) = (1 + Cx)^3(1 - {}^1/_5 Cx) \tag{4.3}$$

and

$$f_\perp(x) = (1 + Cx)(1 - {}^1/_3 Cx) \tag{4.4}$$

where the coefficient C is empirically expressed as

$$C = {}^1/_2\{\tanh[(N - N^*)/\Delta] + 1\} \tag{4.5}$$

with two adjustable parameters N^* and Δ. The functions $f_r(d_e/L_e)$ and $f_\perp(d_e/L_e)$ vary only from 1 to 2.56 and from 1 to 1.6, respectively, in the range of allowable values of d_e/L_e. Thus, D_r and $D_\perp$ are rather insensitive to the parameters N^* and Δ.

The longitudinal diffusion coefficient $D_\parallel$ along the polymer end-to-end axis was treated on the basis of the hole theory, which had originally been used to deal with the self-diffusion of small molecules in liquid by Cohen and Turnbull.[35] The jamming effect on $D_\parallel$ arising from head-on collisions of polymer chains was formulated to be[4,5]

$$D_\parallel = \hat{D}_{\parallel 0} \exp(-V^*_{ex} c') \tag{4.6}$$

where $\hat{D}_{\parallel 0}$ is $D_\parallel$ without the jamming effect and V^*_{ex} the excluded volume between the *critical hole* and a hindering chain. The critical hole was assumed to be similar in shape to the fuzzy cylinder, and V^*_{ex} was expressed in terms of the wormlike cylinder parameters and one adjustable parameter λ^*, the *similarity ratio* of the critical hole to the fuzzy cylinder.

The zero-shear viscosity η_0 of the polymer solution was expressed as[4,5]

$$\eta_0 = \eta^{(S)} + \hat{\eta}_0^{(V)} + \chi^2 \frac{c' k_B T}{10 D_r} \tag{4.7}$$

Here, $\eta^{(S)}$ is the pure solvent viscosity, $\hat{\eta}_0^{(V)}$ is the zero-shear viscosity induced by the friction between polymer and solvent, and the third term is the zero-shear viscosity induced by the orientational entropy loss of polymer chains under the shear flow. The last term is expressed by D_r and a hydrodynamic factor χ. Equation 4.7 without the factor χ^2 was originally derived by Doi and Edwards[1] for rodlike polymer solutions.

In general, the four hydrodynamic quantities $\hat{D}_{r0}$, $\hat{D}_{\perp 0}$, $\hat{D}_{\parallel 0}$, and $\hat{\eta}^{(V)}$ are affected by intra- and intermolecular hydrodynamic interactions (HI). Recently, we[9] attempted to correct these quantities for the intermolecular HI, proposing the following equations for $\hat{\eta}^{(V)}$, $\hat{D}_{r0}$, and $\hat{D}_{\parallel 0}$:

$$\hat{\eta}^{(V)} = (1 - {}^3/_4 \gamma\chi^2)[\eta]\eta^{(S)} c(1 + k'_{HI}[\eta]c) \tag{4.8a}$$

$$k_B T/\hat{D}_{r0} = (k_B T/D_{r0})(1 + k'_{HI}[\eta]c) \tag{4.8b}$$

and

$$k_B T/\hat{D}_{\parallel 0} = (k_B T/D_{\parallel 0})(1 + k'_{HI}[\eta]c) \tag{4.8c}$$

Here, $[\eta]$ is the intrinsic viscosity, c is the polymer mass concentration, D_{r0} and $D_{\parallel 0}$ are the rotational and longitudinal diffusion coefficients at infinite dilution,

respectively, and γ is the hydrodynamic parameter relating D_{r0} to $[\eta]$ by

$$c'k_BT/D_{r0} = {}^{15}/_{2}c[\eta]\eta^{(S)}\gamma \qquad (4.9)$$

The last factor $(1 + k'_{HI}[\eta]c)$ on each right-hand side of eq 4.8 considers the intermolecular HI effect up to the linear order of c, and the coefficient k'_{HI} represents the strength of the intermolecular HI.[36] Similarly, $\hat{D}_{\perp 0}$ may be written as

$$k_BT/\hat{D}_{\perp 0} = (k_BT/\hat{D}_{\perp 0})(1 + k'_{HI}[\eta]c) \qquad (4.8d)$$

with the transverse diffusion coefficient $D_{\perp 0}$ at infinite dilution. The hydrodynamic quantities $[\eta]$, D_{r0}, $D_{\|0}$, $D_{\perp 0}$, γ, and χ including the intramolecular HI effect can be calculated by hydrodynamics (cf. ref 5).

It turns out from eqs 4.1, 4.7, and 4.8 that the Huggins coefficient k' defined by the equation

$$\eta_0 = \eta^{(S)}\{1 + [\eta]c + k'([\eta]c)^2 + \cdots\}$$

consists of the entanglement term k'_{EI} and the intermolecular HI term k'_{HI}:

$$k' = k'_{HI} + k'_{EI} \qquad (4.10)$$

From eqs 4.1 and 4.7, the former term is given by

$$k'_{EI} \equiv {}^{3}/_{2}\gamma\chi^2\beta^{-1/2}\frac{L_e{}^4N_A}{[\eta]ML}f_r(d_e/L_e)(F_{\|0}/F_{r0})^{1/2} \qquad (4.11)$$

Here L is the polymer contour length and $F_{\|0}$ and F_{r0} are factors related to the effects of the *intra*molecular HI on $D_{\|0}$ and D_{r0}, respectively. In ref 4, the factors $F_{\|0}$ and F_{r0} are given as explicit functions of the axial ratio p ($\equiv L/d$) and N of the polymer.

As explained in the Appendix, the dynamical mean-field theory, originally proposed by Doi et al.[19] for rodlike polymer solutions, may be applied to systems of the fuzzy-cylinder model. This theory provides the following expression of the dynamic structure factor $\hat{S}(k,t)$ at a sufficient small magnitude of the scattering vector k (cf. eqs A.8, A.9, and A.11):

$$\hat{S}(k,t) = \frac{RT}{M_0(\partial\Pi/\partial c)}\exp(-D_mk^2t) \qquad (4.12)$$

Here RT is the gas constant multiplied by the absolute temperature, M_0 is the monomer molecular weight, $\partial\Pi/\partial c$ is the derivative of the osmotic pressure Π with respect to c, and D_m is the mutual (or cooperative) diffusion coefficient given by

$$D_m \equiv {}^{1}/_{3}(D_{\|} + 2D_{\perp})(M/RT)(\partial\Pi/\partial c)(1 - \bar{v}c) \qquad (4.13)$$

It is noted that the last factor $1 - \bar{v}c$ in eq 4.13, where $\bar{v}$ is the partial specific volume of the polymer, takes into account the effect of the solvent backflow in the polymer-diffusion process,[37] which is neglected in the Appendix. The front factor ${}^{1}/_{3}(D_{\|} + 2D_{\perp})$ is regarded as the self-diffusion coefficient D_s of the polymer, and eq 4.13 will be used later to extract it from D_m.

B. Huggins Coefficient. The Huggins coefficients k' of 10 PHIC samples in 25 °C toluene listed in the sixth column of Table 1 are plotted against the Kuhn statistical segment number N in Figure 8 by filled circles. We can see that k' takes a minimum around $N = 1$. A similar dependence of k' was previously observed for PHIC in DCM.[9]

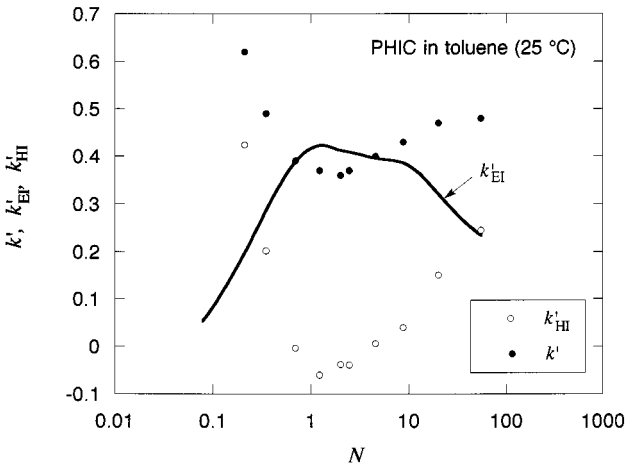

Figure 8. Huggins coefficient k' and the contributions of the entanglement interaction k'_{EI} and of the intermolecular hydrodynamic interaction k'_{HI} for toluene solutions of PHIC: (●) k, (○) k'_{HI}, and the solid curve, k'_{EI} calculated by eq 4.11.

The solid curve in Figure 8 shows the N dependence of k'_{EI} calculated by eq 4.11 for PHIC in toluene at 25 °C. Here, we used the wormlike cylinder parameters, $M_L = 740$ nm^{-1}, $q = 37$ nm, and $d = 1.6$ nm (cf. Table 2), and $N^* = \Delta = 4$ in the function $f_r(d_e/L_e)$ being previously determined for DCM solutions of PHIC.[8,9] The value of $[\eta]M$ in eq 4.11 was calculated by the theory of Yamakawa, Fujii, and Yoshizaki[14,15] for the wormlike cylinder model with the same M_L, q, and d. The calculated k'_{EI} takes a maximum in an intermediate N region, and becomes small at both $N \lesssim 1$ and $\lesssim 10$. At $N = 0.022$ ($=d/2q$), the axial ratio p of the polymer becomes 1 and k'_{EI} reduces to zero, while in the coil limit ($N \to \infty$) k'_{EI} tends to 0.102.[9]

We estimated the contribution k'_{HI} of the intermolecular HI for each PHIC sample in toluene by subtracting the theoretical k'_{EI} (the solid curve in Figure 8) from experimental (total) k' (the filled circles in Figure 8), according to eq 4.10. The unfilled circles in Figure 8 show the estimated k'_{HI} for the PHIC samples studied in toluene. The values of k'_{HI} are much smaller than k'_{EI} at N ranging from 1 to 10, demonstrating less importance of the intermolecular HI in k'. However, k'_{HI} in the smaller and larger N regions becomes larger, and the intermolecular HI plays an important role in k'.

Several workers[38−42] calculated k'_{HI} for hard spheres (which correspond to $N = 0.022$ for PHIC), and obtained values from 0.69 to 1. On the other hand, effective medium theories[43−45] for Gaussian coils with sufficiently large N provided k'_{HI} from 0.38 to 0.695. Furthermore, according to the theory of Muthukumar and Edwards,[46] k'_{HI} for long rodlike polymers should be much smaller than that for Gaussian coils. Thus, k'_{HI} for stiff-chain polymers with relatively small N but still sufficiently large p may be smaller than the coil limit values (0.38−0.695). The results of k'_{HI} shown in Figure 8 seem to be consistent with all of those theoretical predictions.

In a narrow intermediate N range in Figure 8, k'_{HI} values are slightly negative. These negative values are physically unreasonable and may come from the approximations to the hydrodynamic parameters γ, χ, $F_{\|0}$, or F_{r0} appearing in eq 4.11. Since the entanglement contribution is predominant in this N range, a small

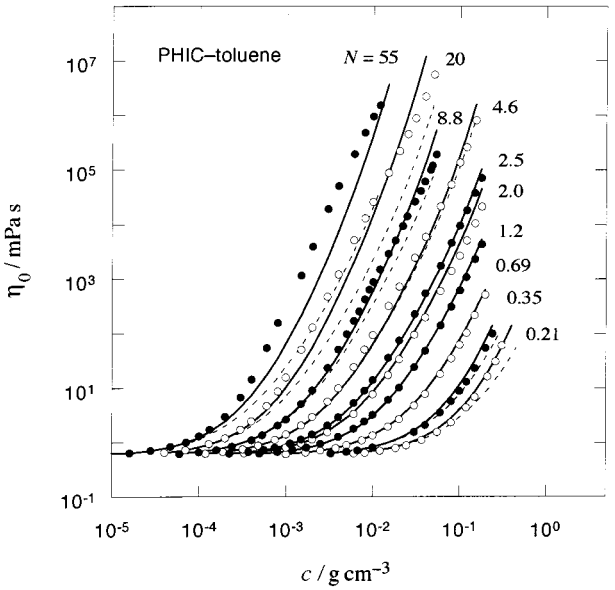

Figure 9. Comparison between experiment and the fuzzy-cylinder-model theory of zero-shear viscosities for toluene solutions of PHIC: solid and dashed curves, theoretical values with and without considering the intermolecular hydrodynamic interaction, respectively.

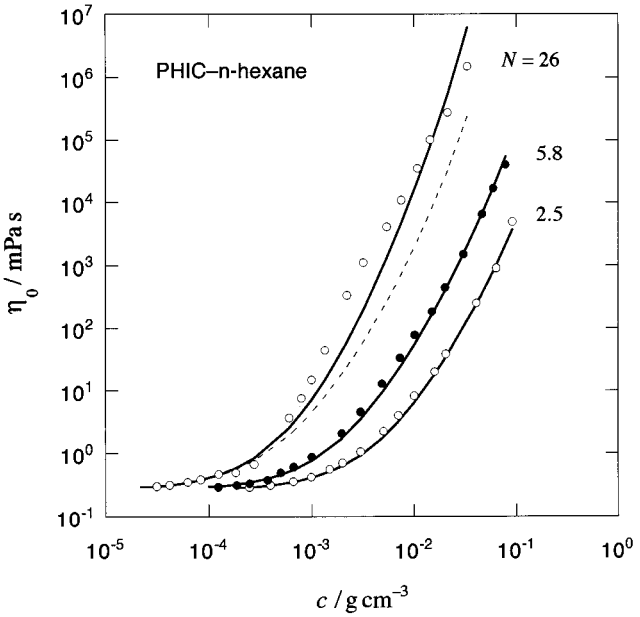

Figure 10. Comparison between experiment and the fuzzy-cylinder-model theory of zero-shear viscosities for *n*-hexane solutions of PHIC: solid and dashed curves, theoretical values with and without considering the intermolecular hydrodynamic interaction, respectively.

error in k'_{HI} can be shown not to seriously affect theoretical results of η_0 mentioned below.

C. Zero-Shear Viscosity. To calculate η_0 by combining eqs 4.1−4.9, we must determine the three adjustable parameters, λ^* in V^*_{ex} in eq 4.6 and N^* and Δ in eq 4.5. In part 2 of this series of papers,[9] we have shown that experimental η_0 data for DCM solutions of PHIC (with $N \leq 15$) are satisfactorily fitted by the fuzzy-cylinder-model theory with $\lambda^* = 0.03$ and $N^* = \Delta = 4$. Here, we use the same parameters for toluene and *n*-hexane solutions of PHIC. Other parameters contained in eqs 4.1−4.9 can be calculated from M for each PHIC sample listed in Table 1 and the wormlike-cylinder parameters in the corresponding solvents listed in Table 2; experimental values were used for the solvent viscosities $\eta^{(S)}$.

Figure 9 compares experimental η_0 data for 25 °C toluene solutions of 10 PHIC samples with the fuzzy-cylinder-model theory. The solid curves in the figure represent theoretical values of η_0 including the effect of the intermolecular HI. The values of k'_{HI} shown in Figure 8 were used for the calculations except at $1.2 \leq N \leq 2.5$, where k'_{HI} takes slightly negative values. Since the negative k'_{HI} is unreasonable, we have chosen k'_{HI} to be zero in this narrow N range; this change of the k'_{HI} value did not essentially alter the theoretical η_0. The theoretical solid curves for the PHIC samples with $N \leq 8.8$ follow closely the experimental data points of toluene solutions over the entire concentration range examined. This demonstrates the validity of the fuzzy-cylinder-model theory for describing the solution viscosity of the semiflexible polymer PHIC with $N \leq 8.8$, confirming the previous conclusion obtained in part 2[9] from the viscosity study on DCM solutions of PHIC.

However, in Figure 9, the agreement between theory (solid curve) and experiment is marginal at $N = 20$ and unsatisfactory at $N = 55$. At $N = 20$, the theory slightly underestimates the experimental results in a semidilute regime at $c \lesssim 1 \times 10^{-2}$ and overestimates those at higher c, while at $N = 55$ the deviation between theory and experiment at $c \lesssim 1 \times 10^{-2}$ is more pronounced.[47]

As shown in Figure 1, the concentration dependence of η_0 for high molecular weight PHIC samples seem to obey a power law at high c, which resembles that for entangled flexible polymer solutions, where the *reptation-like motion* of polymer chains is believed to be important.[1] The reptation-like motion of polymer chains is not incorporated in the theory of the fuzzy-cylinder model explained above, and it may be responsible for the disagreement between the theory and experiment of η_0 at $N = 20$ and 55.

The dashed curves in Figure 9 represent theoretical η_0 with $k'_{HI} = 0$, which ignore the effect of the intermolecular HI. The curve for the smallest N (= 0.21) appreciably deviates downward from the corresponding solid curve and also the data points, indicating that the intermolecular HI plays an important role in the solution viscosity of low molecular weight PHIC, which has already been mentioned when k'_{HI} was compared with k'_{EI} in Figure 8. The good fit of the solid curve to the data points for this sample demonstrates that the effect of the intermolecular HI is appropriately incorporated into the fuzzy-cylinder-model theory explained above. The dashed curve also deviates from the solid curve at $N \geq 8.8$, indicating the intermolecular HI appreciably contributes to η_0 also at high molecular weights of PHIC at high concentrations.

The η_0 data for *n*-hexane solutions are compared with the same theory in Figure 10, where k'_{HI} was taken to be zero at $N = 2.5$ and 5.8, although k'_{HI} calculated by experimental k' were slightly negative. Agreements between experiment and theory are quantitative for $N = 2.5$ and 5.8. On the other hand, the theoretical solid curve for $N = 26$, which includes the intermolecular HI effect, deviates from the data points in a manner similar to the case of toluene solutions with $N = 20$ in Figure 9. The dashed curve ignoring the effect of the intermolecular HI further deviates from the data points for $N = 26$.

In Figure 3, the solid curve for toluene and *n*-hexane solutions and the dot−dash curve for DCM solutions, of PHIC sample M-2 with $N = 2.5$, were actually drawn

by using the fuzzy-cylinder-model theory. In the calculation, the value of q used is 21 nm for DCM solutions and 37 nm for toluene and *n*-hexane solutions (cf. Table 2), while k'_{HI} used is 0.1 for DCM solutions and zero for toluene and *n*-hexane solutions. The chain stiffness enhances the entanglement effect on the solution viscosity, so that η_0 of toluene and *n*-hexane solutions is higher than that of DCM solutions in an intermediate c region. However, η_0 of DCM solutions catches up with those of toluene and *n*-hexane solutions with increasing the polymer concentration. This is due to the stronger effect of the intermolecular HI in η_0 of DCM solutions.

D. Mutual Diffusion Coefficient. From eq 4.13, the quantity $D_m/[(M/RT)(\partial\Pi/\partial c)(1 - \bar{v}c)]$ is equal to $^1/_3(D_{||} + 2D_\perp)$, which may be compared with the self-diffusion coefficient D_s. The fuzzy-cylinder-model theory can calculate the latter quantity from eqs 4.2 and 4.6 with

$$D_s = {}^1/_3(D_{||} + 2D_\perp) = D_0\frac{(D_{||} + 2D_{||0}) + 2(D_{\perp 0} + 2D_{||0})(D + D_{\perp 0})}{1 + 2(D_{\perp 0}/D_{||0})} \quad (4.14)$$

where $D_{\perp 0}/D_{||0}$ may be calculated in the manner described in the appendix of ref 4 or ref 5. Equations 4.2 and 4.6 contain the four unknown parameters, λ^*, N^*, Δ, and k'_{HI}. We again use the previously determined values $N^* = \Delta = 4$ and $\lambda^* = 0.03$, which fit the fuzzy-cylinder-model theory to η_0 data for DCM, toluene, and *n*-hexane solutions of PHIC with $N \lesssim 20$. The value of k'_{HI} for each sample is calculated from experimental k' listed in Table 1, using eqs 4.10 and 4.11. Although the fit of D_0 data to the Yamakawa−Fujii theory gave $d =$ 2.5 nm (cf. Figure 7), the effective diameter d_e of the fuzzy cylinder and also the hydrodynamic parameter $D_{\perp 0}/D_{||0}$ in eq 4.14 are calculated using the value of d (=1.6 nm) used in the comparison of the viscosity, which is a more realistic value of d for the PHIC chain. On the other hand, for D_0 in eq 4.14, the experimental values shown in Figure 7 are inserted.

The inverse of the osmotic compressibility $\partial\Pi/\partial c$ for DCM solutions of PHIC at 20 °C was measured by Itou et al.[48] by sedimentation equilibrium and also by Jinbo et al.[12] by static light scattering. The results were favorably compared with the scaled particle theory with the hard-core diameter of 1.07 nm and the attractive interaction parameter of −0.35 nm.[12,49] Using the same theory, we estimated $\partial\Pi/\partial c$ for the DCM solutions for which dynamic light scattering measurements were made in this study, and calculated $D_m/[(M/RT)(\partial\Pi/\partial c)(1 - \bar{v}c)]$ with experimental D_m and $\bar{v}$; we used the results of Itou et al.[48] for $\bar{v}$ of PHIC in 20 °C DCM [$\bar{v} = (0.992 + 0.0343w)$ cm^3/g, where w is the weight fraction of the polymer in solution].

Figure 11 compares the experimental data of $D_m/[(M/RT)(\partial\Pi/\partial c)(1 - \bar{v}c)]$ with the fuzzy-cylinder-model theory. Agreements between theory and experiment are almost satisfactory for all the four samples examined. We should notice that the theory uses the same adjustable parameters as those used in the viscosity equation in Part 2.[9] Thus, the fuzzy-cylinder-model theory can explain consistently both η_0 and D_m for DCM solutions of PHIC.

The dashed curves in Figure 11 represent the theoretical results at neglecting the effect of the intermolecular HI for samples MO-3 and F-1. Comparison of this figure with Figure 4 for η_0 in ref 9 shows that the

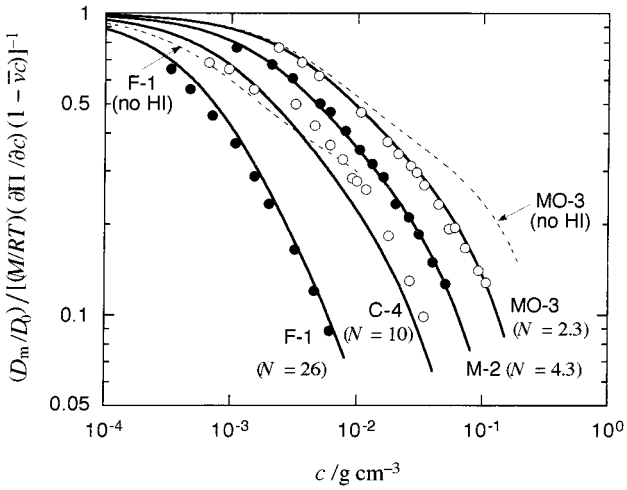

Figure 11. Comparison between experiment and the fuzzy-cylinder-model theory of "self" diffusion coefficients of four PHIC samples in DCM solutions: solid and dashed curves, theoretical values with and without considering the intermolecular hydrodynamic interaction, respectively.

contribution of the intermolecular HI is equally significant on the self-diffusion coefficient $D_s = {}^1/_3(D_{||} + D_\perp)$ and on η_0. However, the entanglement effect is much weaker on D_s than on η_0 or D_r. This reflects the fact that the longitudinal motion of the polymer chain is hardly retarded by the entanglement or jamming in comparison with the rotational motion. Thus, the effect of the intermolecular HI is relatively more important in D_s.

The agreement between the theory and experiment of the translational diffusivity for sample F-1 with $N =$ 26 in DCM seems better than those of viscosities for sample G-2 with $N = 20$ in toluene and for sample JP-2 with $N = 26$ in *n*-hexane. This implies that the range of N where the fuzzy-cylinder-model theory is applicable is wider for the translational diffusivity than for the viscosity. However this must be confirmed by further dynamic light scattering experiments over a wider molecular weight range.

5. Concluding Remarks

As mentioned in section 4A, the basic assumption of the fuzzy-cylinder-model theory is that even above the overlap concentration c^*, local entanglements among polymer chains in solution are easily released to permit each polymer chain to change its conformation much faster than global motions and to make the segment distribution of each chain cylindrically symmetric. On the other hand, the reptation theory for entangled flexible polymer solutions assumes oppositely that local entanglements among polymer chains are stationary and each chain behaves as if it were trapped in a fixed winding tube. We may anticipate that when the conformation of a polymer chain changes from rodlike to coillike (or the Kuhn segment number N of the polymer chain is increased), the polymer dynamics in concentrated solutions changes from the fuzzy-cylinder-like motion to the reptation-like motion. In this connection, it is pertinent to present the following two remarks, one concerning the hydrodynamic parameters derived and the other related to the crossover from the semiflexible to flexible regimes.

In this publication along with the previous ones,[4,5,8,9] we have shown that the fuzzy-cylinder-model theory

Table 3. Hydrodynamic Parameters for Stiff-Chain Polymer Solutions

polymer	solvent	q/nm	λ^*	N^*	Δ	ref
PHIC	DCM (20 °C)	21	0.06	4	4	8[a]
			0.03	4	4	9
	toluene (25 °C)	37	0.03	4	4	
	n-hexane (40 °C)	37	0.03	4	4	
xanthan	0.1 M NaCl (25 °C)	120	0.11	6	4	4[a]
schizophyllan	water (25 °C)	200	0.13	6	4	4[a]

[a] Analyzed without considering the intermolecular HI.

with the intermolecular HI effect included describes almost quantitatively experimental data for η_0 and D_s for polymer samples with $N \lesssim 20-26$. This theory contains the three hydrodynamic parameters λ^*, N^*, and Δ along with the wormlike chain parameters M_L, d, and q, and the intermolecular hydrodynamic interaction parameter k'_{HI}. Since M_L, d, q, and k'_{HI} can be estimated from dilute solution data separately, only the former three are the adjustable parameters in the fuzzy-cylinder-model theory. Table 3 summarizes the values of the hydrodynamic parameters so far determined. For PHIC, a single set of the parameter values suffices to describe the data for the three solvent systems consistently. It is noted that the inclusion of the intermolecular HI has a significant effect on the concentration dependence of η_0 for PHIC solutions, reducing the value of λ^* largely. This parameter takes into account the retardation of the translational motion of the chain due to head-on collision with the surrounding molecules and may be related to their molecular geometry and segment distributions, but at present no molecular theoretical interpretation is available for this relation. On the other hand, N^* and Δ are related to the small correction factors f_r and $f_\perp$ (cf. eqs 4.3−4.5), and their approximate values are sufficient. For schizophyllan and xanthan, the entanglement effect is overwhelming, and the intermolecular HI effect is too small to argue its significance.

On the other hand, this theory fails to describe quantitatively the viscosity data for PHIC with $N \gtrsim 20$. The N value 20 may be the limit, above which the fuzzy-cylinder-model theory becomes inaccurate. At these large N, η_0 of PHIC solutions follows a power law at higher concentration, like entangled flexible polymer solutions. However, it was not a universal function of $c[\eta]$ (cf. Figure 4 of ref 8), though this universality is a prerequisite to the scaling argument for semidilute solutions of flexible polymers.[1,50] Furthermore, as shown in Figure 2 and also in Figure 3 of ref 8, the power law exponent (=4) in the molecular weight dependence of η_0 for toluene and DCM solutions of PHIC is larger than the prediction of the reptation theory (=3).[1] Indeed such larger exponents are characteristic of stiff-chain polymers as noted before.[21,22] Thus, we see that the dynamics of PHIC with $N \gtrsim 20$ in concentrated solutions cannot be described by the reptation theory and is still affected by some chain-stiffness effects. Neither the fuzzy-cylinder-model theory nor the reptation theory is relevant to describe the viscosity behavior of PHIC solutions with $N \gtrsim 20$.

Acknowledgment. This work was supported by a Grant-in-Aid for Scientific Research (No. 07651110) from the Ministry of Education, Science, Sports, and Culture of Japan. A. T. thanks Yamashita Construction Design Inc. for the Chair-Professorship at Ritsumeikan University.

Appendix. Dynamical Mean-Field Theory for the Dynamic Structure Factor

We extend Doi et al.'s theory[19] of dynamic light scattering for rodlike polymer solutions to semiflexible polymer solutions, using the fuzzy cylinder model. Let $f(\mathbf{r},\mathbf{a};t)$ be the single-particle distribution function of a fuzzy cylinder whose position of the center of mass and unit vector parallel to the cylinder axis are $\mathbf{r}$ and $\mathbf{a}$, respectively, at a time t. According to Doi et al., we write the kinetic equation governing the time evolution of $f(\mathbf{r},\mathbf{a};t)$ as[51]

$$\frac{\partial f}{\partial t} = \nabla_{\mathbf{r}}\cdot[D_{\parallel}\mathbf{aa} + D_{\perp}(\mathbf{I} - \mathbf{aa})]\cdot[\nabla_{\mathbf{r}} f + f\,\nabla_{\mathbf{r}}(h + W)] + D_r\nabla_{\mathbf{a}}\cdot[\nabla_{\mathbf{a}} f + f\,\nabla_{\mathbf{a}}(h + W)] \quad \text{(A.1)}$$

where $D_{\parallel}$, $D_{\perp}$, and D_r are the longitudinal, transverse, and rotational diffusion coefficients, respectively, and $\nabla_{\mathbf{r}}$ and $\nabla_{\mathbf{a}}$ are the gradient operators in the three-dimensional space and on the two-dimensional unit spherical surface, respectively. In the last two terms of eq A.1, h is the potential of an external field and W is the potential of the molecular field created by surrounding polymers. In a mean-field approximation, W is calculated from an *effective* interaction potential $w_{eff}(\mathbf{r} - \mathbf{r}',\mathbf{a},\mathbf{a}')$ between two fuzzy cylinders taking the configurations $(\mathbf{r},\mathbf{a})$ and $(\mathbf{r}',\mathbf{a}')$ by

$$W = \int d\mathbf{r}' \int d\mathbf{a}'\, w_{eff}(\mathbf{r} - \mathbf{r}',\mathbf{a},\mathbf{a}')c'f(\mathbf{r}',\mathbf{a}';t) \quad \text{(A.2)}$$

where c' is the number concentration of fuzzy cylinders in the solution.

The smoothed-density theory for the second virial coefficient[52] writes $w_{eff}(\mathbf{r} - \mathbf{r}',\mathbf{a},\mathbf{a}')$ as

$$w_{eff}(\mathbf{r} - \mathbf{r}',a,a') = \beta_{eff}\int dR = \int d\mathbf{R} \int dz\, d\mathbf{b} \int dz'\, d\mathbf{b}'\, \rho(z,\mathbf{b})\rho(z',\mathbf{b}')\delta[\mathbf{R} - (\mathbf{r} + z\mathbf{a} + \mathbf{b})]\delta[\mathbf{R} - (\mathbf{r}' + z'\mathbf{a}' + \mathbf{b}')] \quad \text{(A.3)}$$

Here β_{eff} is the *effective* strength of the excluded-volume interaction between segments (or monomers) belonging to two fuzzy cylinders, $\delta(\mathbf{x})$ is the delta function, and $\rho(z, \mathbf{b})$ is the average segment density of the fuzzy cylinder written in terms of the cylindrical coordinates $(z,\mathbf{b})$, where the center of mass and cylinder axis of the fuzzy cylinder are chosen as the origin and polar axis, respectively.

As shown by Doi et al., the fluctuation−dissipation theorem gives the dynamic structure factor $\hat{S}(k,t)$ in the form

$$\hat{S}(k,t) = \frac{N_0}{4\pi}\int_t^{\infty} dt' \int d\mathbf{a}\; s_{\mathbf{k}}(\mathbf{a}) \exp(-t'\Omega_{\mathbf{k}})\theta_{\mathbf{k}} s_{\mathbf{k}}(\mathbf{a}) \quad \text{(A.4)}$$

where N_0 is the degree of polymerization, $N_0 s_{\mathbf{k}}(\mathbf{a})$ is the Fourier transform of the average segment density of the fuzzy cylinder $\rho(z,\mathbf{b})$, and $\theta_{\mathbf{k}}$ and $\Omega_{\mathbf{k}}$ are the operators defined by

$$\theta_{\mathbf{k}} s_{\mathbf{k}}(\mathbf{a}) = \{D_{\parallel}(\mathbf{k}\cdot\mathbf{a})^2 + D_{\perp}[\mathbf{k}^2 - (\mathbf{k}\cdot\mathbf{a})^2] - D_r\nabla_{\mathbf{a}}\} s_{\mathbf{k}}(\mathbf{a}) \quad \text{(A.5)}$$

and

$$\Omega_{\mathbf{k}} s_{\mathbf{k}}(\mathbf{a}) = \theta_{\mathbf{k}}\int d\mathbf{a}'\, [\delta(\mathbf{a} - \mathbf{a}') + (c'/4\pi)w_{\mathbf{k}}(\mathbf{a},\mathbf{a}')] s_{\mathbf{k}}(\mathbf{a}') \quad \text{(A.6)}$$

with $w_{\mathrm{eff},\mathbf{k}}(\mathbf{a},\mathbf{a}')$ being the Fourier transform of $w(\mathbf{r}-\mathbf{r}',\mathbf{a},\mathbf{a}')$. From eq A.3, $w_{\mathrm{eff},\mathbf{k}}(\mathbf{a},\mathbf{a}')$ is written in the form

$$w_{\mathrm{eff},\mathbf{k}}(\mathbf{a},\mathbf{a}') = \beta_{\mathrm{eff}} N_0^{\,2} s_{\mathbf{k}}(\mathbf{a}) s_{-\mathbf{k}}(\mathbf{a}') \qquad (A.7)$$

Since $\Omega_{\mathbf{k}}$ is an integro-differential operator with a mathematically complex structure, it is in general difficult to obtain the eigenvalues and eigenfunctions and thus to evaluate $\hat{S}(k,t)$ by eqs A.4 and A.6. However, as demonstrated by Doi et al., this mathematical problem can be solved in the special case of $k \to 0$. The final result at $k \to 0$ is simply written as

$$\hat{S}(k,t) = \frac{N_0}{1+b} \exp[-D_s(1+b)k^2 t] \qquad (A.8)$$

where $b \equiv \beta_{\mathrm{eff}} N_0^2 c'$ and D_s is the averaged self-diffusion coefficient of the fuzzy cylinder defined by

$$D_s \equiv {}^1/_3(D_{\|} + 2D_{\perp}) \qquad (A.9)$$

At $t = 0$, $\hat{S}(k,t)$ reduces to the static structure factor, which is related to the osmotic pressure Π of the solution at $k \to 0$ by[53]

$$\frac{1}{\hat{S}(k,0)} = (M_0/RT)(\partial\Pi/\partial c) \; (k \to 0) \qquad (A.10)$$

where M_0 is the monomer molecular weight, RT is the gas constant multiplied by the absolute temperature, and c is the polymer mass concentration. Comparing eqs A.8 and A.10, we have the following relation:

$$1 + b = (M_0/RT)(\partial\Pi/\partial c) \qquad (A.11)$$

References and Notes

(1) Doi, M.; Edwards, S. F. *The Theory of Polymer Dynamics*; Clarendon Press: Oxford, England, 1986.
(2) Schaefer, D. W.; Han, C. C. In *Dynamic Light Scattering*; Pecora, R., Ed.; Plenum Press: New York and London, 1985.
(3) Fujita, H. *Polymer Solutions*; Elsevier: Amsterdam, 1990.
(4) Sato, T.; Takada, Y.; Teramoto, A. *Macromolecules* **1991**, *24*, 6220.
(5) Sato, T.; Teramoto, A. *Adv. Polym. Sci.* **1996**, *126*, 85.
(6) Sato, T.; Ohshima, A.; Teramoto, A. *Macromolecules* **1994**, *27*, 1477.
(7) Fujiyama, T.; Sato, T.; Teramoto, A. *Acta Polym.* **1995**, *46*, 445.
(8) Ohshima, A.; Kudo, H.; Sato, T.; Teramoto, A. *Macromolecules* **1995**, *28*, 6095.
(9) Sato, T.; Ohshima, A.; Teramoto, A. *Macromolecules* **1998**, *31*, 3094.
(10) Itou, T.; Chikiri, H.; Teramoto, A.; Aharoni, S. M. *Polym. J.* **1988**, *20*, 143.
(11) Murakami, H.; Norisuye, T.; Fujita, H. *Macromolecules* **1980**, *13*, 345.
(12) Jinbo, Y.; Sato, T.; Teramoto, A. *Macromolecules* **1994**, *27*, 6080.
(13) Green, M. M.; Khatri, C. A.; Reidy, M. P.; Levon, K. *Macromolecules* **1993**, *26*, 4723.
(14) Yamakawa, H.; Fujii, M. *Macromolecules* **1974**, *7*, 128.
(15) Yamakawa, H.; Yoshizaki, T. *Macromolecules* **1980**, *13*, 633.
(16) Ohshima, A. Ph.D. Thesis, Osaka University, 1997.
(17) Norisuye, T.; Tsuboi, A.; Teramoto, A. *Polym. J.* **1996**, *28*, 357.
(18) Berne, B. J.; Pecora, R. *Dynamic Light Scattering*; John Wiley & Sons: New York, 1976.
(19) Doi, M.; Shimada, T.; Okano, K. *J. Chem. Phys.* **1988**, *88*, 4070.
(20) Enomoto, H.; Einaga, Y.; Teramoto, A. *Macromolecules* **1984**, *17*, 1573.
(21) Enomoto, H.; Einaga, Y.; Teramoto, A. *Macromolecules* **1985**, *18*, 2695.
(22) Takada, Y.; Sato, T.; Teramoto, A. *Macromolecules* **1991**, *24*, 6215.
(23) Ferry, J. D. *Viscoelastic Properties of Polymers*, 3rd ed.; John Wiley & Sons: New York, 1980.
(24) For dilute *n*-hexane solutions of PHIC, Kubota and Chu[28] observed nonlinearity in $g^{(2)}(t)$ and positive k^2 dependence of Γ/k^2, and analyzed them by the dynamic light scattering theory of Fujime and co-workers[55, 56] for the wormlike chain.
(25) Although not shown in Figure 4, data points of $\ln[g^{(2)}(t) - 1]$ exhibited a weak upswing in a very short time region. This upswing was observed at any θ and c examined for this sample and also sample F-1, and a similar behavior was reported by Konishi et al.[57] for dilute polystyrene solutions. Here we neglected this upswing to evaluate Γ.
(26) Russo, P. S.; Karasz, F. E.; Langley, K. H. *J. Chem. Phys.* **1984**, *80*, 5312.
(27) Yamakawa, H.; Fujii, M. *Macromolecules* **1973**, *6*, 407.
(28) Kubota, K.; Chu, B. *Macromolecules* **1983**, *16*, 105.
(29) Godfrey, J. E.; Eisenberg, H. *Biophys. Chem.* **1976**, *5*, 301.
(30) Edwards, S. F.; Evans, K. E. *J. Chem. Soc., Faraday Trans. 2* **1982**, *78*, 113.
(31) Teraoka, I.; Hayakawa, R. *J. Chem. Phys.* **1988**, *89*, 6989.
(32) Teraoka, I.; Hayakawa, R. *J. Chem. Phys.* **1989**, *91*, 2643.
(33) Teraoka, I.; Ookubo, N.; Hayakawa, R. *Phys. Rev. Lett.* **1985**, *55*, 2712.
(34) Teraoka, I. Ph.D. Thesis Thesis, University of Tokyo, 1988.
(35) Cohen, M. H.; Turnbull, D. *J. Chem. Phys.* **1959**, *31*, 1164.
(36) In eqs (4.8), we have used "the one-constant approximation"[9] where all the coefficients representing the strengths of the intermolecular HI in $\hat{D}_{\mathrm{r0}}$, $\hat{D}_{\|0}$, and $\hat{\eta}_0^{(\mathrm{V})}$ are equal to each other.
(37) Fujita, H. *Polymer Solutions*; Elsevier: Amsterdam, 1990; Chapter 8.
(38) Peterson, J. M.; Fixman, M. *J. Chem. Phys.* **1963**, *39*, 2516.
(39) Batchelor, G. K.; Green, J. T. *J. Fluid Mech.* **1972**, *56*, 401.
(40) Bedeaux, D.; Kapral, R.; Mazur, P. *Physica* **1972**, *76*, 247.
(41) Batchelor, G. K. *J. Fluid Mech.* **1977**, *83*, 97.
(42) Freed, K. F.; Muthukumar, M. *J. Chem. Phys.* **1978**, *69*, 2657.
(43) Freed, K. F.; Edwards, S. F. *J. Chem. Phys.* **1975**, *62*, 4032.
(44) Muthukumar, M. *J. Phys. A: Math Gen.* **1981**, *14*, 2129.
(45) Muthukumar, M. *J Chem. Phys.* **1983**, *79*, 4048.
(46) Muthukumar, M.; Edwards, S. F. *Macromolecules* **1983**, *16*, 1475.
(47) Similar trend can be observed also for PHIC solutions with $N = 4.6$ and 8.8, although the deviation of the theory from experimental data is very small.
(48) Itou, T.; Sato, T.; Teramoto, A.; Aharoni, S. M. *Polym. J.* **1988**, *20*, 1049.
(49) Sato, T.; Jinbo, Y.; Teramoto, A. *Macromolecules* **1997**, *30*, 590.
(50) de Gennes, P. G. *Macromolecules* **1976**, *9*, 594.
(51) In the Appendix, we neglect the effect of the solvent backflow in the diffusion process just for simplicity. This effect can be taken into account simply by multiplying the factor $1 - \bar{v}c$ ($\bar{v}$, the partial specific volume of the polymer; c, the polymer mass concentration) to the diffusion coefficients $D_{\|}$ and $D_{\perp}$.[37]
(52) Yamakawa, H. *Modern Theory of Polymer Solutions*; Harper & Row: New York, 1971.
(53) Fujita, H. *Polymer Solutions*; Elsevier: Amsterdam, 1990; Chapter 5.
(54) Itou, T.; Teramoto, A. *Macromolecules* **1988**, *21*, 2225.
(55) Fujime, S.; Maruyama, M. *Macromolecules* **1973**, *6*, 237.
(56) Maeda, T.; Fujime, S. *Macromolecules* **1981**, *14*, 809.
(57) Konishi, T.; Yoshizaki, T.; Yamakawa, H. *Macromolecules* **1991**, *24*, 5614.

MA9909298